Indian Journal of

Engineering

Flow Physics Analysis around three-bladed Savonius Wind Rotor

Sharma KK[1], Biswas A[2], Gupta R[3]

1.Assoc. Prof., Deptt. of Mechanical Engg, NIT Silchar, India, Email: kksharma1313@rediffmail.com
2.Assistant Professor, Deptt. of Mechanical Engg, NIT Silchar, India, Email: agnibis@yahoo.co.in
3.Director, NIT Srinagar, India, Email: rguptanitsri@gmail.com

※**Corresponding Author:** Dr.K.K.Sharma, Department of Mechanical Engg., N.I.T.Silchar Email ID: kksharma1313@rediffmail.com

Citation
Sharma KK, Biswas A, Gupta R. Flow Physics Analysis around three-bladed Savonius Wind Rotor. *Indian Journal of Engineering*, 2014, 11(25), 6-17

ABSTRACT

In this paper, 2D flow through a three-bucket Savonius rotor is studied by Fluent 6.0 computational fluid dynamics software. The flow physics encompassed in the flow around the rotor is analyzed with the help of pressure, velocity and vorticity contours. The objective of the present study is to optimize the performance of this design of Savonius rotor under different overlap conditions through the evaluation of its flow physics at these conditions. The overlap in the three-bucket Savonius rotor has been increased with the help of nuts and bolts times (like 15.38% & 16.88%). In CFD various flow parameters such as dynamic pressure, static pressure, turbulence intensity and vorticity are studied.

Keywords: Savonius rotor, CFD, flow physics

1. INTRODUCTION

Wind is an environmental friendly renewable energy source whose continual tapping for power generation will improve the present scenario of climate change from green gas emissions .It is estimated that roughly 10 million MW of energy are continuously available in the earth's wind. Wind energy is converted into mechanical power by wind turbines and then converted into electricity with the help of generator. Wind turbines are broadly classified into two

types: Horizontal Axis Wind Turbine (HAWT) and Vertical axis Wind turbine (VAWT). VAWT rotor's flow physics is studied in the present paper. Savonius rotor is also a type of VAWT rotor. The concept of Savonius rotor is based on the principle developed by Flettner, which is formed by cutting a cylinder into two halves along the central plane and then moving to two semi-cylindrical surfaces sideways along the cutting plane, so that the cross-section resembled the letter 'S' (Savonius, 1931). Experiments (Newman, 1974) had been done on Savonius rotor with variable gap (Katsuya and Toshio, 2001), simulated numerically the flow over a two-bucket Savonius rotor by solving 2D finite volume equations using an upwind scheme for unstructured mesh. Their results showed good matching with the experimental values of power coefficient and aerodynamic coefficients. The performance of a three-bucket Savonius rotor had been evaluated by (Debnath et al., 2009) in combination with three-bladed combined Savonius-Darrieus rotor with overlap variations using Fluent 6.0 CFD software. The result showed good matching of computational and experimental power coefficient for all overlap conditions (Cochran et al. 2004) numerically simulated the flow patterns in and around a two-bucket Savonius rotor of thirteen different configurations to optimize the blade configurations by using Reynolds-stress 5-equation turbulence model. They further concluded that 2D CFD simulation was sufficient as the blades rotate in the same plane as the approaching wind, thereby reducing the computational time and effort. In the present paper, objective of the present study is to optimize the performance of this design of Savonius rotor under different overlap conditions through the evaluation of its flow physics at these conditions.

2. PHYSICAL MODEL

The buckets of the rotor are 8 cm in chord, 3mm in thickness and 20 cm in height. Rotor is fixed to the shaft using nut and bolt arrangement. Ball bearing is used to support the central shaft of the rotor at the base. Washers and nuts having the knurled surfaces have been used to change the overlap as seen in figure A. Overlap is the distance of the inner edge of the bucket from the axis of rotation when the arc of the bucket is a full semi-circle. Different overlap conditions like 15.38% & 16.88%. The central shaft of the rotor has been taken as 1.5cm in diameter and 2.5cm thick. The dimension of the base has been taken as 7cm wide and 2.4cm thick.

3. CFD FORMULATION

CFD simulations are carried out using Fluent 6.0 software. The conservative forms of Continuity equation (eq^{n}1) and Navier-Stokes equations (eq^{n}s 2 & 3) for the incompressible unsteady flow is solved by the inbuilt functions of the Fluent 6.0 software. Likewise, the continuity and turbulence closure equations are also solved by the software. For the three-bucket Savonius rotor, two-dimensional steady computational domain is considered. For pressure-velocity coupling of the flow, the Semi-Implicit Pressure Linked Equations (SIMPLE) algorithm [6] is used to solve all the scalar variables of flow. For the turbulent closure, k-epsilon SST model of Fluent software is used, which is solved using the green-gauss cell based gradient option. The model of turbulence closure predicts well for flow having strong adverse pressure gradients like that of the flow past Savonius wind rotor. Second order discretization scheme [7] for the continuity, momentum, and turbulence equations is selected in order to improve the accuracy of predictions.

$$\frac{\partial u_i}{\partial x_i} = 0 \tag{1}$$

The momentum equation in terms of relative velocity, v_r can be written as

$$\frac{\partial}{\partial t}(\rho \vec{v}_r) + \nabla.(\rho \vec{v}_r \vec{v}_r) + \rho(2\vec{\omega}\vec{v}_r + \vec{\omega}\vec{\omega}r) = -\nabla p + \rho \vec{g} + \nabla.(\bar{\bar{\tau}}) \tag{2}$$

Where p is the static pressure, $\bar{\bar{\tau}}$ is the stress tensor of a Newtonian fluid, $\rho\vec{g}$ is the gravity force, $\rho(2\vec{\omega}\vec{v}_r)$ is the Coriolis force and $\rho(\vec{\omega}\vec{\omega}r)$ is the centrifugal force.

According to the eddy viscosity concept of the Stokes' hypothesis for Newtonian fluids, the Reynolds stress tensor, $\bar{\bar{\tau}}$ can be expressed as

$$\bar{\bar{\tau}} = \mu[(\nabla\vec{v} + \nabla\vec{v}^T) - \frac{2}{3}\nabla.\vec{v}I] \tag{3}$$

4. FLOW PHYSICS ANALYSIS

The contour plots at different overlap have been given as follows. The overlap is given by washer having thickness of 1.2mm or combination of washers.

4.1. Contour plots evaluations at 15.38% overlap

For the 15.38% overlap (Figure 1) the formation of wake can be visualized. The length of wake can be visualized, and its shape is more erratic and curved shape. A spot of blue colour on the downstream side shows that a velocity of
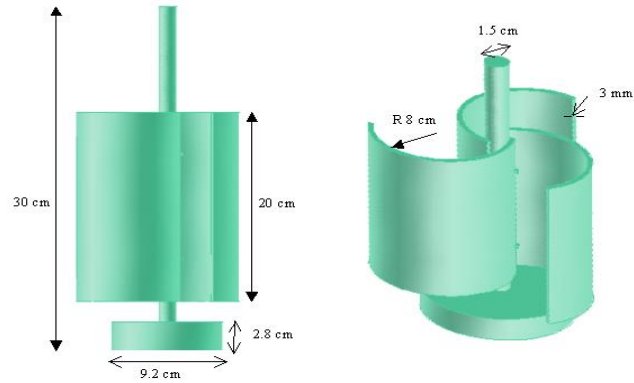
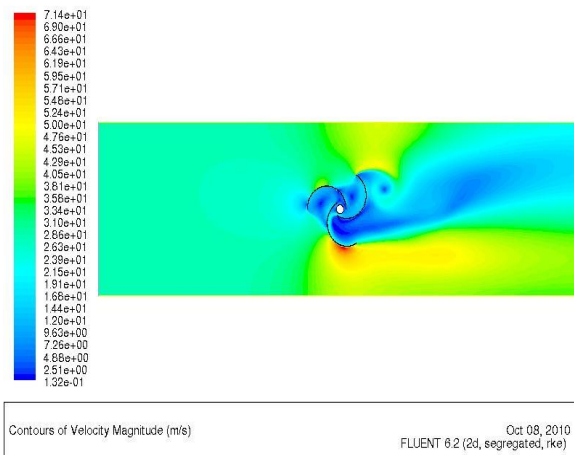**Figure A**

Physical model of the three-bucket Savonius Rotor

Figure 1

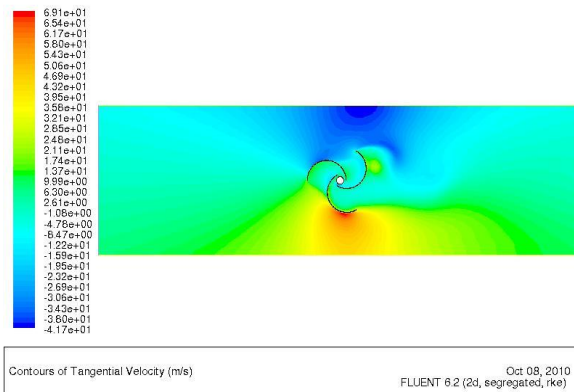Variation of velocity magnitude along the upstream and down streamside of Savonius rotor (At 15.38% overlap)

Figure 2

Variation of tangential velocity along upstream and downstream side of Savonius rotor (At 15.38% overlap)
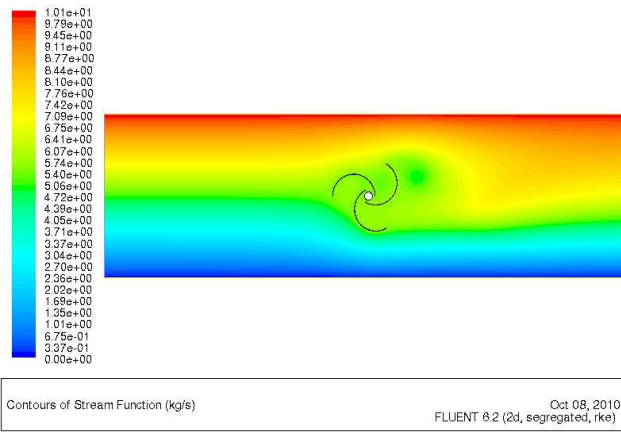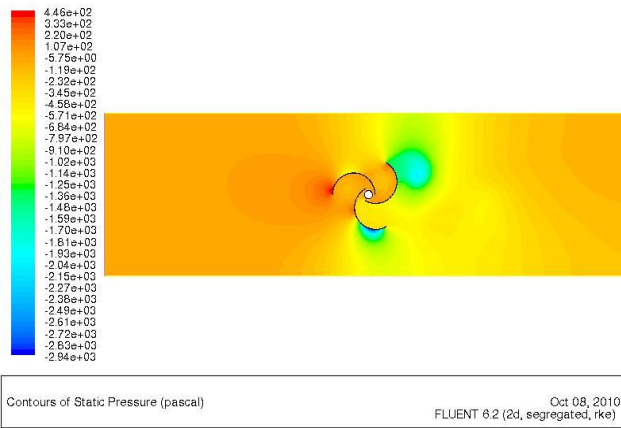
Contours of Stream Function (kg/s)   Oct 08, 2010
                                                            FLUENT 6.2 (2d, segregated, rke)

Figure 3
Variation of stream function along upstream and downstream side of Savonius rotor (At 15.36% overlap)

Contours of Static Pressure (pascal)   Oct 08, 2010
                                                            FLUENT 6.2 (2d, segregated, rke)

Figure 4
Variation of static pressure along upstream and downstream side of Savonius rotor (At 15.38% overlap)

Contours of Dynamic Pressure (pascal)   Oct 08, 2010
                                                            FLUENT 6.2 (2d, segregated, rke)

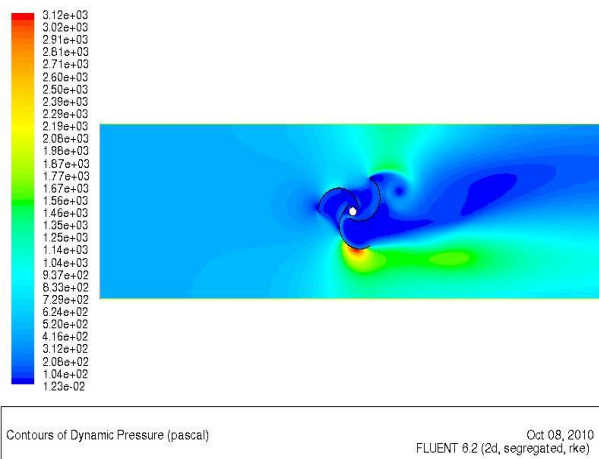**Figure 5**
Variation of dynamic pressure along upstream and downstream side of Savonius rotor (At 15.38% overlap)

Contours of Total Pressure (pascal)   Oct 08, 2010
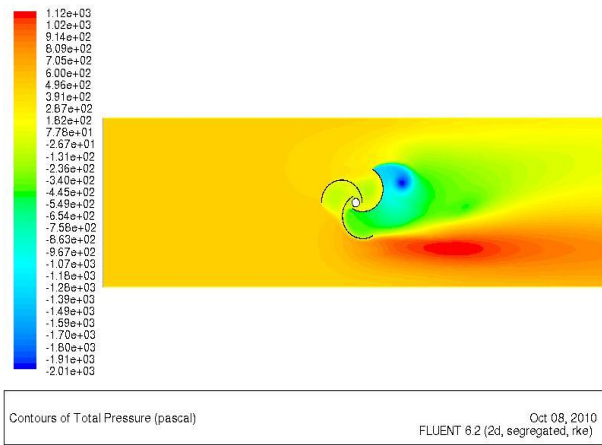   FLUENT 6.2 (2d, segregated, rke)

Figure 6

Variation of total pressure along upstream and downstream side of Savonius rotor (At 15.38% overlap)

Contours of Turbulence Kinetic Energy (k) (m2/s2)   Oct 08, 2010
                                    FLUENT 6.2 (2d, segregated, rke)
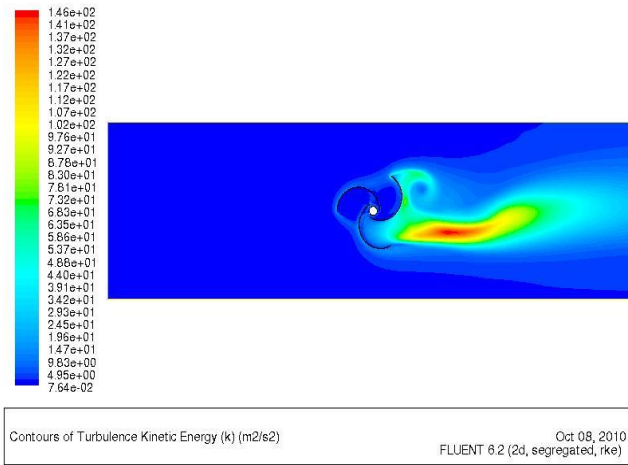
Figure 7

Variation of turbulence Kinetic Energy along upstream and downstream side of Savonius rotor (At 15.38% overlap)

Contours of Turbulence Intensity (%)   Oct 08, 2010
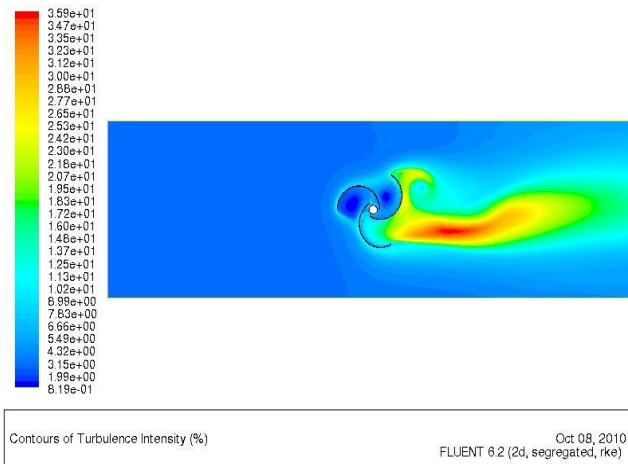   FLUENT 6.2 (2d, segregated, rke)

Figure 8

Variation of turbulence intensity along upstream and downstream side of Savonius rotor (At 15.38% overlap)
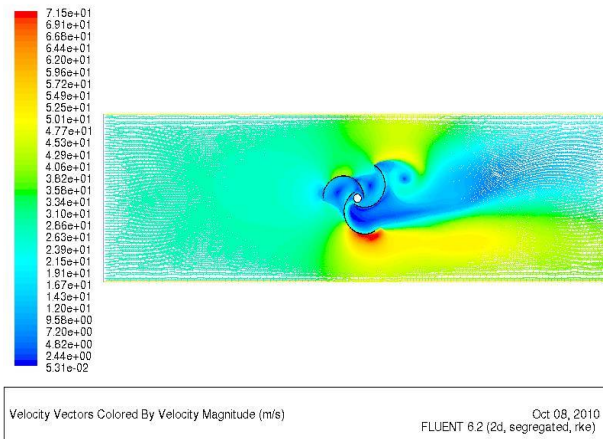
Figure 9

Variation of velocity magnitude along upstream and downstream side of Savonius rotor (At 15.38% overlap)
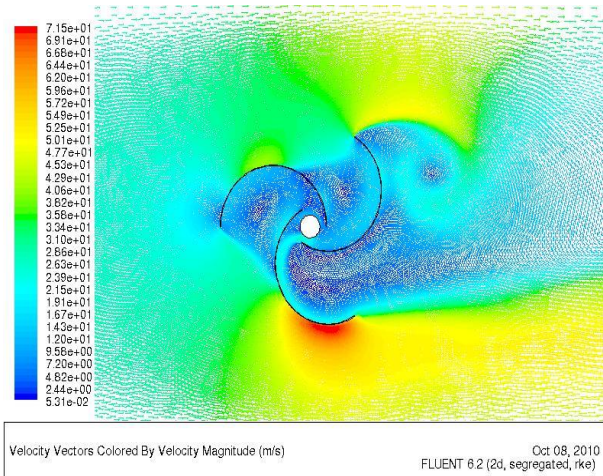

Figure 10

Variation of velocity magnitude along upstream and downstream side of Savonius rotor (At 15.38% overlap)

0.132 m/s exists at that place. In figure 2 the tangential velocity can be seen by the red colour shows that there is maximum tangential velocity is of negative magnitude and lies between of between 38 m/s to 41.7 m/s. In Figure 3, the value of the stream function on the left side of the rotor is seen by red colour and its value lies between 9.11 kg/s and 10.1 kg/s can be seen on the left side of wind rotor while on the right side of wind rotor there is blue colour showing the stream function between 0 to 0.675 kg/s. In Figure 4, the deep red colour is seen in the above diagram shows maximum pressure seen by red colour having maximum static pressure 446 Pa whereas light green colour seen in the downstream side shows a static pressure –0.00102 Pa. Static pressure increases as the wind goes toward the tip of the front blade and the value of static pressure is more at the tip of the blade seen by red colour, and there is decrease in velocity in the downstream side, which shows that there is lift in the three – bladed Savonius wind turbine.

In Figure 5, the maximum dynamic pressure can be visualized by red colour having the magnitude of 3120 Pa and by yellow colour (approximate 2190 Pa) and the minimum pressure on the downstream side is seen by deep blue colour between the pressure 0.0123 Pa to 104 Pa. At some places pressure is seen by green color (having the magnitude of 1350 Pa and the wake is seen by deep blue colour having the magnitude of 0.0123 Pa .The typical shape in the wake region of the above diagram have the pressure of 0.0123 Pa. The shape and size of the wake in the above diagram is quite different from the shape and size of earler wakes in the case of overlap of (two washers, three washers. Around the wake the high pressure zone is prevailed. Low velocity of wind in wake creates more power in the shaft. In figure 6, the maximum value of total pressure have the magnitude of 1120 Pa seen by red colour

whereas lower value of total pressure seen by green colour having the magnitude -549 Pa to -236 Pa is seen in downstream side, whereas total pressure of -2010 Pa is seen by deep blue colour in the diagram. The pressure seen by red colour has the magnitude of 1120 Pa.

In Figure 7, minimum turbulence kinetic intensity is seen by deep blue colour 0.0764 m^2/s^2 whereas on the downstream side by deep red colour by 0.0146 m^2/s^2. Whereas by deep green colour turbulence kinetic intensity between 56.6 m^2/s^2 and 67.6 m^2/s^2. The shape of the turbulence kinetic energy is as seen by the curved shape seen in figure. Difference of value of turbulence kinetic energy at different places can be seen in the above diagram. The above peculiar shape of turbulence kinetic intensity can be seen from the above diagram. From Figure 8, the minimum turbulence intensity is seen by deep blue color by 0.0819 % whereas maximum intensity is seen by deep red color having turbulence intensity between 34.7% to 35.6%. The above type of closed curve of turbulence intensity zone can be seen in the above type of diagram. Higher turbulence intensity zone is surrounded by lower turbulence intensity zone as seen in figure.

From Figure 9, maximum velocity seen by red colour is 71.5 m/s while the velocity seen by blue colour is between 0.0531 m/s to 4.82 m/s. Visualisation seen by yellow colour is between 47.7 to 62.5 m/s. Deep sky colour shows velocity variation between 31 to 38 m/s. In the above diagram different types of velocity variation in the wake can be visualized when three bladed Savonius rotor is rotating with overlap of 5washers (15.38%). The wake is surrounded by high velocity of wind. The variation of width and length of wake can be seen in downstream side as seen in figure. Separation of flow can be seen one at the surfaces of one of the blade, while separation of flow can be seen at the tip of the other blade as seen from the diagram. Two vortices or eddies can be seen in between the blades while circular vortex or eddy can be seen outside the turbine along the downstream side. Probably Karman type of vortex sheet can be visualized if correct velocity contours can be obtained.

From figure 10, highest velocity can be seen at the tip one of the blade having velocity of 71.5 m/s. Two vortices or eddies are formed in between the blades, while one vortex at outside the blade can easily be visualized in the above diagram. Probably Von Karman type of vortex sheet can be easily seen in the downstream side of the wind tunnel. Vortices of low velocity are surrounded by the high fluid velocity. Flow separation at the wall of the blades and flow separation at the tip can be seen from the figure, and vortex shedding can be seen.

4.2. Contour plots evaluations at 16.88% overlap

From figure 11, the maximum velocity seen by red colour is 71.6 m/s to 75.4 m/s whereas vorticity like figure can be seen in the downstream side and velocity between 0.015 m/s to 4.93 m/s can be visualized in the downstream side. Two vortices can be seen inside the blades while one of the vortex can be seen outside the rotor. The shape i.e. length and width of wake can be outside the rotor, whose shape is different from the wake of the Savonius rotor of earlier rotor i.e. the Savonius rotor with overlap i.e. with four washers. From figure 12, the contours of tangential velocity can be seen from the above diagram. Blue colour shows less magnitude of tangential velocity having the magnitude of -44 m/s, while the red colour shows maximum value of tangential velocity having the magnitude of 73 m/s. The tangential velocity between 11.8 m/s to 22.8 m/s. is seen by green colour at different places. From figure 13, the maximum stream function by red colour 10.3 m/s to 10.9 m/s is seen by red colour whereas minimum value of stream function is seen by blue colour 0.0 m/s to 0.6 m/s. Whereas stream function by blue colour is between 4.46 to 5.66 kg/s is seen by the diagram whereas two types of vortices one inside the blade and other outside wind rotor in the downstream side can be easily visualized on downstream side. Variation in the path of the streamlines can be seen in the diagram.

From figure 14, three vortices are being seen in the above diagram, two vortices are between the blades and one vortices are being seen on the downstream side which is clearly visible on the downstream side, and streamline variations can be directly visualized on the downstream side. The lowest magnitude have the value equal to 2.07 kg/s can be seen on one side of the rotor , while the highest value of stream function can be seen by red colour having the value 10.9 kg/s. Two vortices can be seen inside the blades while one vortex outside the rotor can be seen from the diagram. From figure 15, the maximum value of static pressure is seen by two red colour having the value 243 Pa and 423 Pa whereas variation is seen by −298 to −138 Pa can be seen by orange colour and light green colour. Decrease in static pressure from upstream side to downstream side shows that there is lift in three- bladed vertical axis wind turbine.

From figure 16, the maximum dynamic pressure 3480 Pa (seen by red colour) whereas minimum dynamic pressure is by 0.0164 Pa (seen by blue colour). Pressure seen by blue colour shows dynamic pressure 0.0164 Pa , whereas the maximum dynamic pressure at one of the tip of blade surface can be seen by red colour having the value 3480 Pa .One vortex type structure can be seen outside the rotor , and the value of dynamic pressure seen by blue colour can be seen by deep blue colour having the value of 0.0164 Pa. Von-Karman type of figure can be seen in the downstream side of the wind-tunnel The shape and size of the wake is different from the shape and size of the wake found for the three-bladed Savonius rotor with overlap of four washers (15.38%).
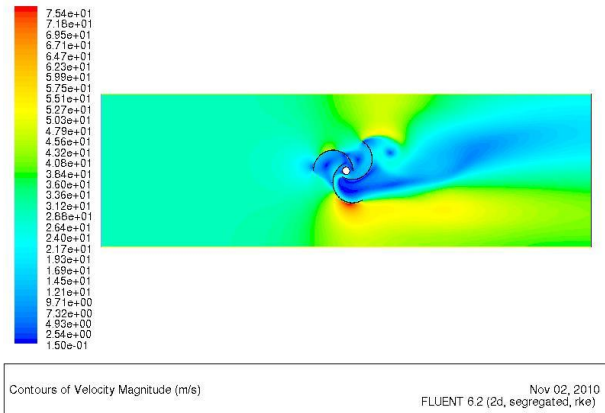
Figure 11

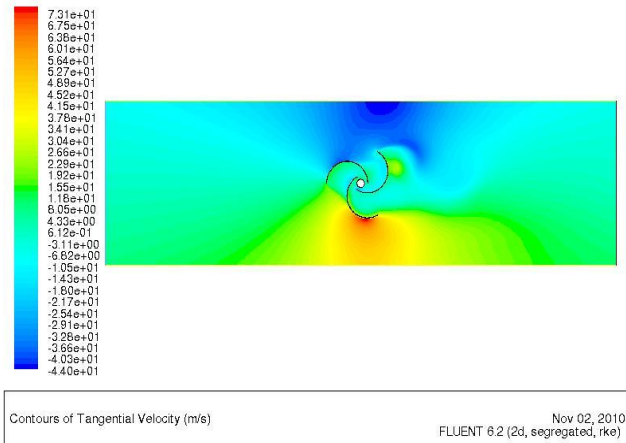Variation of velocity magnitude along upstream and downstream side of Savonius rotor (At 16.88% overlap)

Figure 12

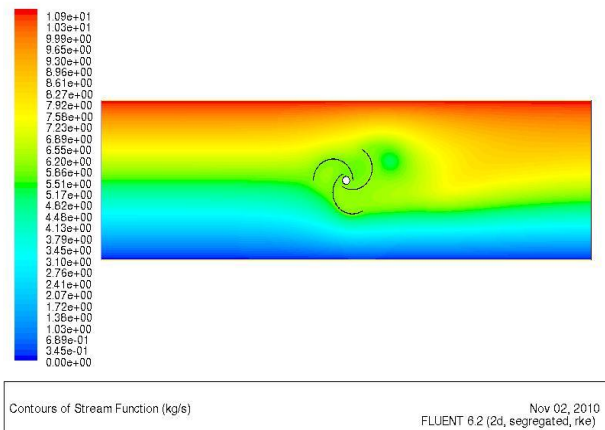Variation of tangential velocity along upstream and downstream side of Savonius rotor (At 16.88% overlap)

Figure 13

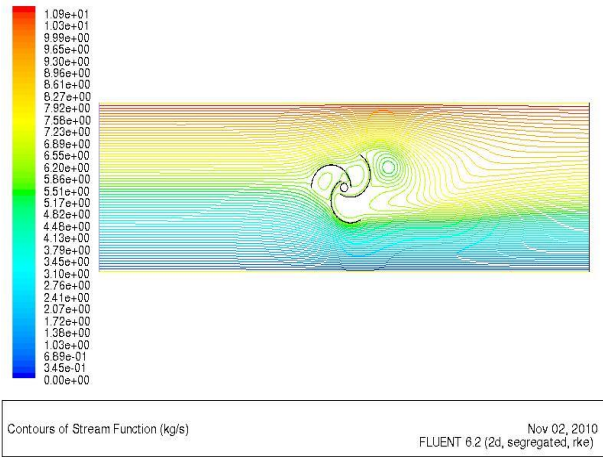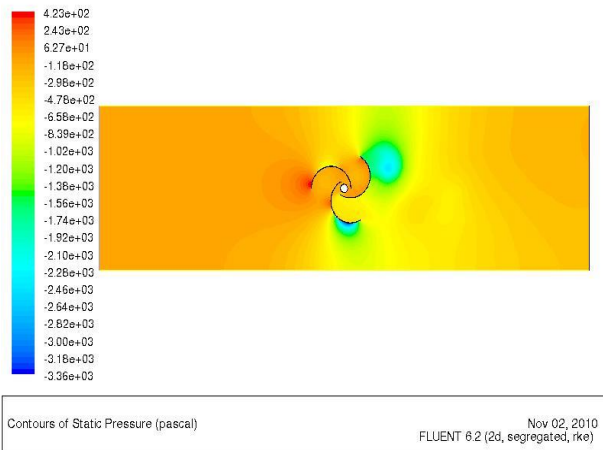Variation of stream function along upstream and downstream side of Savonius rotor (At 16.88% overlap)

Figure 14

Variation of contours of stream function along upstream and downstream side of Savonius rotor (At 16.88% overlap)

Figure 15

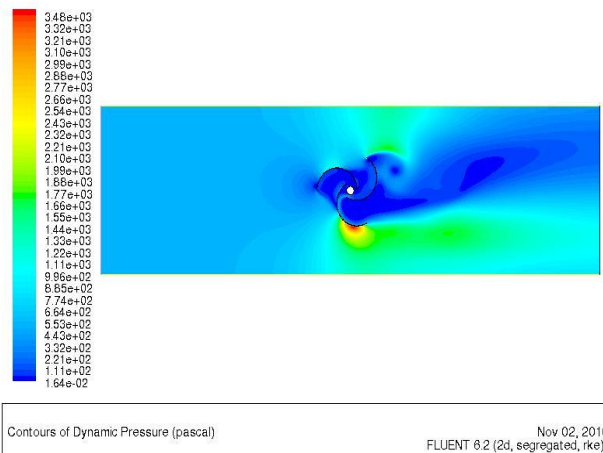Variation of static pressure   along upstream and downstream side of Savonius rotor (At 16.88% overlap)

Figure 16

Variation of static pressure along upstream and downstream side of Savonius rotor (At 16.88% overlap)
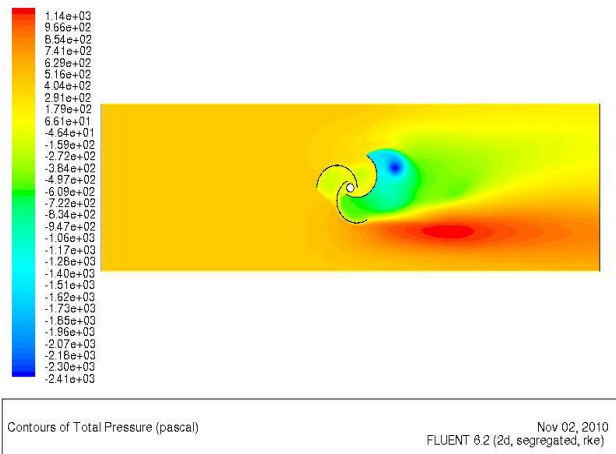
Figure 17
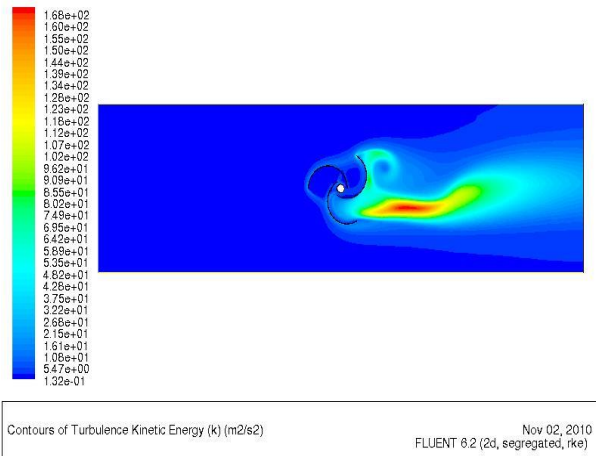Variation of total pressure along upstream and downstream side of Savonius rotor (At 16.88% overlap)

Figure 18
Variation of turbulence kinetic energy along upstream and downstream side of Savonius rotor (At 16.88% overlap)
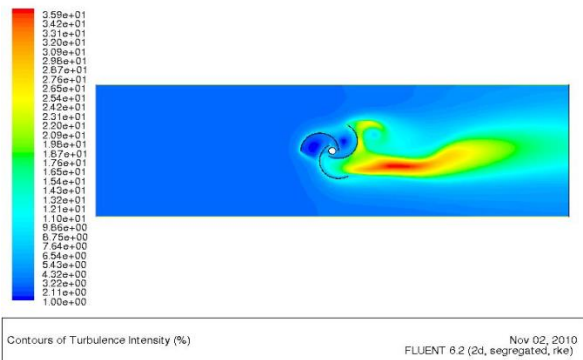

Figure 19
Variation of turbulence intensity along upstream and downstream side of Savonius rotor (At 16.88% overlap)
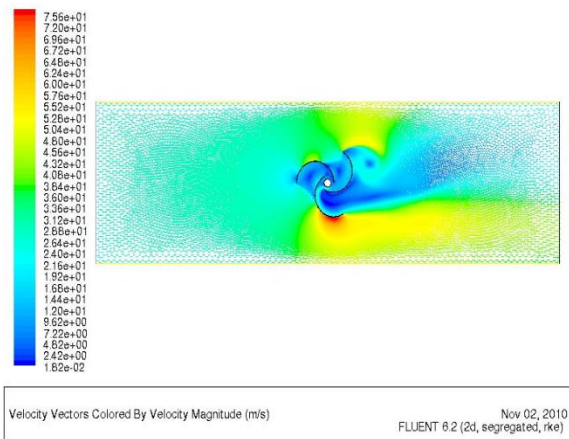
Figure 20
Variation of velocity magnitude along upstream and downstream side of Savonius rotor (At 16.88% overlap)
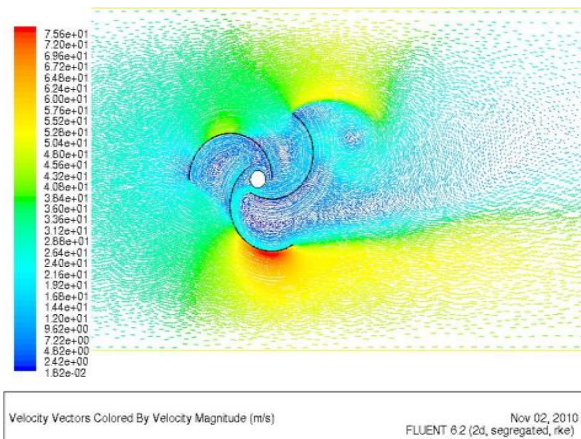

Figure 21
Variation of velocity magnitude along upstream and downstream side of Savonius rotor (At 16.88% overlap)

From figure 17, maximum total pressure seen by red colour shows total pressure in the range of 629 Pa to 1140 Pa. The blue colour shows the variation between −2410 Pa to − 2070 Pa. The variations of total pressure in the green colour are in between -7220 to -2720 Pa as seen in figure. From figure 18, the turbulence kinetic intensity shows the minimum turbulence intensity 0.132 m^2/s^2, wheras maximum value of turbulence kinetic intensity can be seen by deep red colour as seen by curve in the above diagram, which is surrounded by the turbulent flow having low kinetic energy. The maximum value of the kinetic energy seen in figure has the value of 168 m^2/s^2. Turbulence kinetic energy decreases as moving away from the three-bladed Savonius wind turbine along the downstream side.

From figure 19, the maximum turbulence intensity 1 % to 5.43 %   whereas figure seen by red colour shows the turbulence intensity in the range of 33.1 % to 35.9 %. The length of the maximum turbulence intensity zone (seen by red colour) can be seen from the figure whose value decreases as we go away from the three-blades Savonius wind turbine along the downstream side. The different types of the curved shape can be seen in the downstream side as we go away from the three-bladed Savonius wind turbine. From figure 20, velocity at the inlet is approximately 26.6 m/s, whereas in the downstream side is seen by blue colour 0.0182 m/s to 4.82 m/s. The maximum velocity seen by red colour is seen as 72 m/s to 75.6 m/s. In the above type of diagram, the shape and size of the wake is different from the shape and size of wake of the earlier diagram. The width of wake becomes thin after some distance from the three bladed rotor, after that the width of the wake increases and becomes wider, and after some time low velocity zone decreases and higher value of the wind velocity comes in the flow-field. From figure 21, separated layer of fluid flow can be seen passing through the curved concave shape of fluid flow. These separated shear layers can be seen by

light blue color. Flow separated from the tip of the front blade can be seen from the figure, and after leaving the tip surfaces it touches the tip of the next blade, and after that vortex formation is happened.

5. CONCLUSION

From the above study it has been concluded that

1. The contour plot of velocity magnitude of the Savonius rotor the velocity decreases from upstream to downstream side of the rotor. This drop shows that there is power extraction from the wind by rotor.
2. The contour plots of static pressure of the Savonius rotor shows that static pressure decreases from upstream to downstream side of rotor which results in useful lift of rotor.

More correct flow-visualisation can be studied in 3-D study by Fluent Software.

REFERENCES

1. Savonius SJ. The S-rotor and its application. *Journal of Mechanical Engg.*, 1931, 5, 333-337
2. Newman BG. Measurement on a Savonius rotor with variable gap *Proceeding Shebrook University Symposium on wind energy*, Sherbrook Canada, 1974, 116
3. Katsuya I, Toshio S. Simulation of flow around rotating Savonius turbines. *Proceedings of the sixth National Symposium on Computational Fluid Dynamics*, 2001, 691-694
4. Debnath BK, Biswas A, Gupta R. Computational fluid dynamics analysis of a combined three-bucket Savonius and three-bladed Darrieus rotor at various overlap conditions. *Journal of Renewable and Sustainable energy*, 2009, 1, 110-14
5. Cochran BC, David B, Taylor SJ. A three tiered approach for designing and evaluating performance characteristics of novel WECS. *AIAA Paper No. 2004-1362*, 2004
6. Patankar SV. Numerical Heat Transfer and Fluid Flow (*Hemisphere, Taylor & Francis, New York, 1980*)
7. Versteeg HK, Malalasekera W. An Introduction to Computational Fluid Dynamics: The Finite Volume Method (*Longman Scientific and Technical Paper Series, New York, 1995*)